WP15ER-PR(17) 17293

D Galassi et al.

Flux expansion effect on turbulent transport in 3D global simulations

Preprint of Paper to be submitted for publication in
Nuclear Materials and Energy

This work has been carried out within the framework of the EUROfusion Consortium and has received funding from the Euratom research and training programme 2014-2018 under grant agreement No 633053. The views and opinions expressed herein do not necessarily reflect those of the European Commission.

Flux expansion effect on turbulent transport in 3D global simulations

D. Galassi[a], P. Tamain[b], C. Baudoin[b], H. Bufferand[b], G. Ciraolo[b], N. Fedorczak[b], Ph. Ghendrih[b], N. Nace[b] and E. Serre[a]

[a] *Aix Marseille Université, CNRS, Centrale Marseille, M2P2 UMR 7340, 13451, Marseille, France*

[b] *IRFM, CEA Cadarache, F-13108 St. Paul-lez-Durance, France*

e-mail address of the corresponding author: davide.galassi@univ-amu.fr

Abstract

The flux expansion effect on the Scrape-Off Layer equilibrium is inspected through TOKAM3X 3D turbulence simulations. Three magnetic equilibria with analytically controlled flux expansion are built, representing respectively a positive, a null and a negative Shafranov shift. Turbulent $E \times B$ fluxes across flux surfaces show similar amplitudes and poloidal distributions in all cases. The ballooning nature of the interchange instability is recovered, with an enhancement of turbulence in the vicinity of the limiter, probably due to a Kelvin-Helmoltz instability. Interestingly, the poloidally averaged density decay length is found to be shorter almost by a factor 2 in the case of flux surfaces compressed at the low-field side midplane, with respect to the opposite case, indicating the presence of unfavourable conditions for the turbulent transport. The difference in the magnetic field line shape is pointed out as a mechanism which affects the turbulent transport across the flux surfaces. Indeed the unstable region has a larger parallel extension when flux expansion in the low-field side is larger. Moreover, the configuration with a lower magnetic shear at the low-field side midplane shows a more unstable behaviour. The role of

this parameter in turbulence stabilization is qualitatively evaluated. The difference in the distribution of transport along the parallel direction is shown to affect also the parallel flows, which are analyzed for the three proposed cases.

1 Introduction

Recently, the fluid turbulence code TOKAM3X [1] has been run in a divertor configuration, in order to analyze the effects of turbulent transport on global flows in a X-point geometry[2]. One peculiarity of the turbulent transport arising from this simulation, is the fact that the turbulent fluxes tend to adapt to the tokamak magnetic geometry. It is shown, indeed, that the cross-field turbulent flux is enhanced where the flux expansion is stronger, so at the top of the machine and at the X-point. Turbulent structures indeed, to first order, tend to be damped when they are not field aligned. In order to follow the flux surface expansion, turbulent structures must therefore propagate with different radial velocities, according to the flux tube radial extension in the physical space. This distance is regulated by the flux expansion, which has thus a direct geometric effect on turbulent fluxes. Analyzing radial fluxes referred to the magnetic flux coordinate, we can actually study the locations where the turbulent transport is more effective. Simulations in divertor configuration[**?**], for example, have shown that the LFS midplane is the location where the turbulent transport across the flux surfaces is most effective.

The scope of this paper is to inspect more deeply the effect of flux expansion on turbulent transport, independently from the direct geometrical effect on cross-field fluxes just described. In other words, we aim to study the effect of a geometric variation in the real space on the turbulence studied in the magnetic space. This work is carried out through numerical simulations with the 3D fluid turbulence code TOKAM3X [1], whose flexibility in the geometry definition allows to model a large variety of magnetic configurations. Some works on this subject have been carried out with other codes considering a single flux tube geometry and the dynamics of seeded blobs[3]. A global approach is instead retained here, with turbulence arising naturally in the plasma edge, caused mainly by the interchange instability, and in the

framework of a realistic three-dimensional geometry.

2 TOKAM3X simulations setup

2.1 Physical model and parameters

The set of equations solved by TOKAM3X, and the associated boundary conditions, can be found in [1]. It is a drift-reduced, electrostatic turbulence model. The ion Larmor radius and the gyrofrequency are used as reference dimensions for the equation normalization. The electric drift velocity is expressed as $\vec{u}_E = (\vec{B} \times \vec{\nabla}\Phi)/B^2$, while the curvature drift velocity is expressed as $\vec{u}^{i/e}_{\vec{\nabla}B} = \pm 2T_{i/e}(\vec{B} \times \vec{\nabla}B)/B^3$, with the sign + for the ions i and − for the electrons e.
For the following analysis, TOKAM3X is run in isothermal mode, with a constant temperature for both species, $T_e = T_i = T_0$, where T_0 is the reference temperature. This means that in our case the plasma density coincides with the static pressure.
Neutral dynamics is not taken into account. This is an important limitation in the study of the SOL physics. Nevertheless, we are trying to understand a basic physical mechanism as the turbulent transport, so not including the neutral dynamics could help us studying this problem at a basic level, being independent from other physical mechanisms. This approach, moreover, can be representative in situations where the neutral dynamics has a lower impact, as for example in the sheath-limited regime. The inclusion of the temperature evolution in the physical model would allow the development of several additional instability mechanisms, as the sheath-driven conducting-wall [4] and the ITG instabilities. The sheath-driven conducting-wall instability could affect the turbulence properties in the SOL region, but its relative importance with respect to interchange turbulence should be limited, as suggested in [4]. ITG turbulence could probably play an important role both in the edge and in SOL plasma. However, since the driving mechanism of the ITG is comparable to the interchange turbulence appearing in the presented simulations, we do not expect ITG turbulence to change qualitatively the results presented in this work.
Four parameters enter in the physical model. Three of them are diffusion coefficients, for density, parallel momentum and vorticity. They are set for the simulation as $D_{N,\Gamma,W} = 0.5 \cdot 10^{-2}\rho_L^2\omega_c$, where ρ_L is the ion Larmor ra-

dius and ω_c the ion gyrofrequency, and they are constant both in radial and poloidal directions. These coefficients determine the efficiency of the collisional transport, and help to damp the turbulent structures having a scale length comparable to the mesh grid. The fourth parameter is the parallel resistivity, and it is set to $\eta_\parallel = 1 \cdot 10^{-5} B_0/(en_0)$, where n_0 is the reference density used for the normalization. The parallel resistivity value determines the collisionality of the plasma, establishing by consequence a relationship between the plasma density and electronic temperature, according to Braginskii's theory [5]. For a tokamak of the size of COMPASS, for example, with a 0.9 T toroidal field and a density $n_0 = 5 \cdot 10^{18}\ m^{-3}$, the chosen value for the parallel resistivity would lead to a temperature $\sim 18\ eV$.
The particle source has a Gaussian shape in the radial direction, with a half-width of $a/16$, where a is the minor radius. It is poloidally and toroidally constant, and it is located at the inner boundary of the domain, in the closed flux surfaces region.

2.2 Analytical geometries used for simulations

We want to inspect the role of flux expansion on turbulent transport and on global equilibrium. Since we aim to study the flux expansion effect at a basic level, our scope is to disentangle it from all the other possible geometrical aspects related to the divertor configuration, as, for example, the poloidal field singularity at the X-point and the presence of the Private Flux Region. For this reason, three analytic magnetic equilibria are built.
A toroidally limited magnetic configuration is used, where the limiter is modelled as infinitely thin and localized poloidally at the bottom of the machine. The minor radius a of the simulated tokamak measures 256 ρ_L, and the aspect ratio is 3.4. The grid resolution used for simulation is $64 \times 512 \times 32$ in r, θ and φ respectively. Simulations are run until turbulence is fully developed, and the average profiles are quasi-constant in time. The simulation time needed to reach the convergence is typically ~ 3 times larger than the confinement time.
The three magnetic equilibria differ in the flux surface shifts. Flux surfaces are circular, but their centre horizontal position R_ψ is shifted according to the following equation:

$$R_\psi(\psi) = R_0 + \Delta(\psi) = R_0 + S \cdot (r(\psi) - a) \tag{1}$$

Where Δ is the Shafranov shift, ψ is the flux surface coordinate, and the shift parameter S for the three simulations is respectively $1/3$, 0 and $-1/3$. These three cases will be named in the following "inner shift", "no shift"and "outer shift"respectively. We define the flux expansion as:

$$f_x(\psi, \theta) = \frac{\left\langle \vec{\nabla}\psi\,(\psi, \theta) \right\rangle_\theta}{\vec{\nabla}\psi\,(\psi, \theta)} \tag{2}$$

With this definition and the chosen parameters for the shift, in the vicinity of the separatrix the value of the flux expansion on the expanded side, in the shifted cases, is twice the value on the compressed side and $4/3$ times the value in the case without shift. The poloidal flux function Ψ is adjusted in order to obtain the same profile of mean safety factor $q(\psi)$ for the three simulations. In particular, $q(\psi)$ has a parabolic shape, with a value around 4 at the separatrix. The toroidal magnetic field is chosen to vary as $1/R$, with a normalized unitary value at the magnetic axis. As a result, the poloidal field has the shape shown in Figure 1.

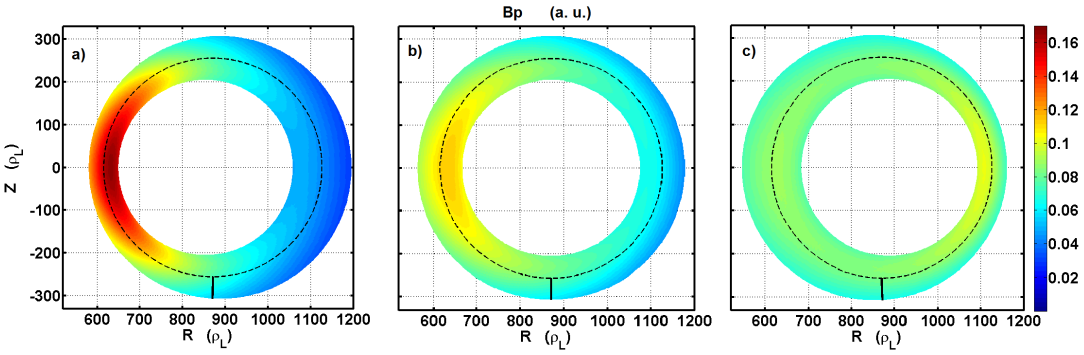

Figure 1: Poloidal magnetic field in the three simulated cases: a) inner shift b) no shift c) outer shift.

One can notice from figure 1 that while in the inner shift case the poloidal field has its maximum at the HFS midplane, for the outer shift case this maximum is located at the LFS midplane. The total connection length is slightly

varied in the three configurations. In particular the outer shift geometry has a connection length at the separatrix around 5% shorter than the case without shift, while for the inner shift configuration this value is roughly 5% bigger.
It must be reminded that the three described cases, and in particular the "inner shift", could differ from realistic magnetic equilibria. The simulations with these configurations must thus be considered as exercises focused on electrostatic turbulence, independently from the MHD stability.

3 Simulation results

In order to characterize the turbulent transport in the presented geometry, we start by analyzing the turbulent $E \times B$ fluxes across the flux surfaces. Averaging in time and in toroidal direction:

$$\left\langle N u_E^{\psi} \right\rangle_{t,\varphi} = \left\langle \tilde{N} \tilde{u}_E^{\psi} \right\rangle_{t,\varphi} + \langle N \rangle_{t,\varphi} \left\langle u_E^{\psi} \right\rangle_{t,\varphi} \tag{3}$$

Where, for a generic field, $\tilde{X} = X - \langle X \rangle_{t,\varphi}$. Turbulent fluxes, identified by the first term in the RHS of (3), are associated with the fluctuating components of the density and electric potential fields. The second term of the RHS in (3) are the mean-field fluxes, associated with the average components of the fields. In contrast with the simulations in divertor geometry [**?**], in the simulations presented here the turbulent fluxes are dominant with respect to the mean-field fluxes. In these simulations, mean-field fluxes are important only at the vicinity of the targets, where the sheath drives strong potential gradients in the poloidal direction.
In order to investigate the turbulence transport efficiency, we show in figure 2 the fluxes measured in the magnetic space, thus normalized by the local value of the flux expansion, as defined in (2).

In the edge region the calculated average radial flux value is $\sim 1.1 \cdot 10^{-2}$ for the three simulations. We can see in figure 2 that in the poloidal direction, turbulent flux distribution does not vary appreciably, and it is mainly centred at the LFS midplane. The geometrical effect of flux expansion, already found in divertor geometry, is confirmed: if the velocities were measured in the physical space, we would find values proportional to the local flux expansion. In the inner shift case then, fluxes at LFS midplane in the ψ

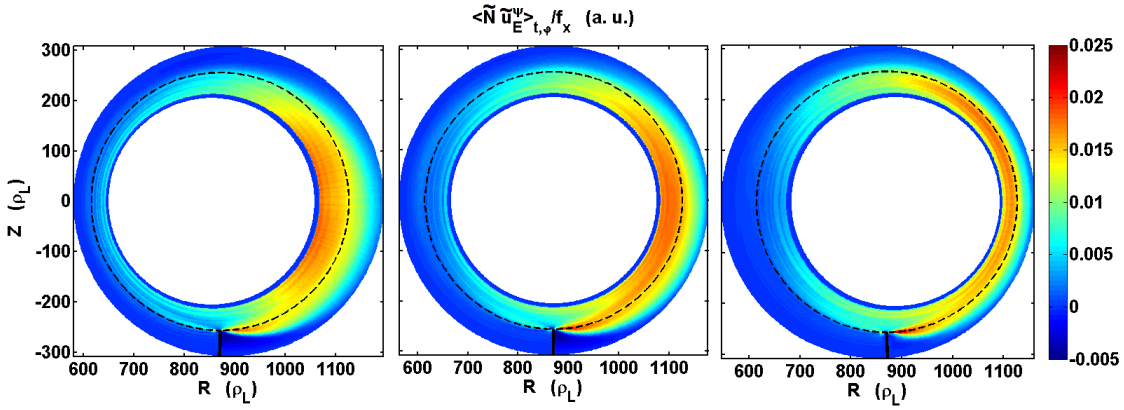

Figure 2: 2D poloidal maps of turbulent flux across the flux surfaces. From left to right: inner shift, no shift and outer shift cases

direction would be, to first order, larger by a factor of two with respect to the outer shift configuration. Studying the fluxes independently from the flux expansion allow us to understand where the turbulent transport is more efficient in crossing the flux surfaces. Flux analysis in magnetic space shows the ballooning-like character of the turbulent flux, typical of the interchange instability, which dominates in this region over the other possible instability mechanisms (Kelvin-Helmoltz, drift waves) for the set of parameter used in these simulations. A considerable outwards turbulent flux can be seen in the three cases in the vicinity of the limiter on the LFS. This turbulence enhancement is likely to be due to a Kelvin-Helmoltz instability, caused by the parallel shear flow between the SOL and the edge region [6]. Indeed, while the parallel flow is almost null in the closed flux surface region, the parallel Mach number passes suddenly to nearly sonic values when crossing the separatrix. The instability criterion expressed in [6] is fulfilled, and the Kelvin-Helmoltz process seems to co-exist with the interchange at the outer side of the limiter in the Scrape-Off Layer (SOL).
Globally, the cross-field turbulent flux does not change appreciably in the three cases. This fact is not astonishing, if we consider that our system is flux-driven, and the particle source is fixed and equal in the three simulations. Interestingly, simulations show that the equilibrium in the radial direction changes in the three cases. Since the cross-field flux is fixed by the input source, not only the density gradient blue but also the local density value adapts according to the efficiency of the turbulent transport. Figure 3 shows

radial profiles for the average density in the three cases.

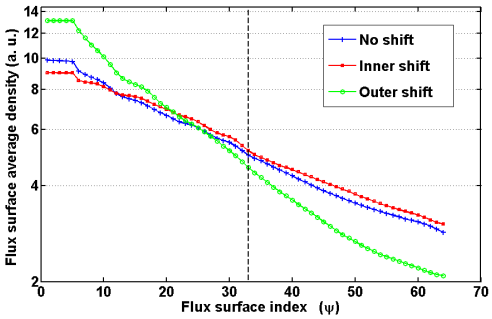

Figure 3: Radial profile of density averaged over the flux surface, remapped on reference flux surfaces.

We notice that density gradients in the magnetic space get steeper for bigger flux compression on the LFS. The case without shift is in an intermediate situation, as could be expected, but its density gradient across the flux surfaces seems actually closer to the inner shift case. Since the poloidally averaged distance between the flux surfaces is almost equal in the three cases, we can compare the decay length of the density in the physical space. After an averaging in time and toroidal direction, the density decay length has been calculated for each poloidal poistion. Then, an average of the decay lengths in the poloidal direction has been obtained. The results of this calculation are shown for the three cases in table 1.

	Inner Shift	No Shift	Outer shift
$\langle \lambda_N \rangle_\theta \, (\rho_L)$	116	85	56
$\langle g \rangle_\parallel \, (a.u.)$	$8.5 \cdot 10^{-4}$	$9.6 \cdot 10^{-5}$	$-6.9 \cdot 10^{-4}$
s	1.6	2.1	3.3

Table 1: Poloidally averaged density decay lengths and geometric parameters affecting turbulence stabilization in the three magnetic configurations.

These results suggest a lower propagation in the SOL of the turbulent structures in the outer shift configuration. Different possible mechanisms can contribute to the turbulence stabilization, and they are discussed in section 4.

4 Stabilization mechanisms

4.1 Field lines average curvature

An important difference between the three configurations, that could affect the turbulent transport, is the shape of the field lines. From a linear analysis done on the physical system of equations solved by the code [7], we know that the destabilizing term for the interchange instability is:

$$g = 4\frac{\partial}{\partial_r}\left(\frac{1}{B}\right) \tag{4}$$

The system is locally unstable when g is positive, so when the local curvature is favourable for the interchange mechanism. If we want to explain the trends of the average density decay length, we need however to calculate an integrated value which characterizes the average turbulent transport over a flux surface. For this reason, we calculate the integral over a poloidal turn in the parallel direction:

$$\langle g \rangle_{\parallel} = \left(\int_0^{2\pi} g\frac{B}{B_p}\mathrm{d}\theta\right) / \left(\int_0^{2\pi} \frac{B}{B_p}\mathrm{d}\theta\right) \tag{5}$$

The calculated value of $\langle g \rangle_{\parallel}$ corresponding to the first flux surface outside the separatrix is reported in table 1. These values vary along the radial direction in a similar way for the three cases, so that the difference between them is almost constant. These results confirm us that the plasma edge is more unstable in the inner shift configuration. Indeed, the g term, which has a cosine shape in θ direction, is shifted towards positive values when the shift parameter S is positive. In our case this happens for the inner shift equilibrium. Here the region with a positive g term is the most extended in the poloidal direction, as a direct effect of the positive shift. Moreover, the parallel length in the unstable region is even longer for the inner shift case, in which the local safety factor is higher at the LFS. This means that globally, a particle will cover a longer path along the field line in an unstable region, so it will be more affected by the cross-field turbulent transport. Indeed, in the case of inner shift, smaller density gradients are needed to drive the same turbulent fluxes, so we can say that it is the most unstable.
The global g parameter shows marked differences between the three cases, so

it could, at least partially, explain the macroscopic differences among them.

4.2 Magnetic shear

The different magnetic shear in the three situations is identified as another possible mechanism which affects the turbulent transport. As mentioned before, the profile of the safety factor $q(\psi)$ is maintained constant over the three simulations. Nevertheless, looking at the dependency of q on the real space radial coordinate, this equality is not valid any more, since the spacing between the flux surfaces is not the same. In particular, the $q(r)$ profile is much steeper for the outer shift case at the LFS midplane. This changes, by consequence, the local magnetic shear. In a toroidal geometry with a circular cross-section, the magnetic shear can be defined as:

$$s(r) = \frac{r}{q(r)} \frac{dq(r)}{dr} \tag{6}$$

Where q is defined as in [8]. Shear values calculated at the LFS midplane, for a radial position correspondent to the separatrix, are shown in table 1. As seen, this global magnetic shear factor varies strongly among the three simulations. A magnetic shear stabilization is reported experimentally in cases of negative magnetic shear [9]. The shearing mechanism due to the magnetic field depends (as explained in [9]) on the alignment between the blobs and the horizontal direction, along which the interchange mechanism acts more efficiently. This is a consequence of the fact that the charge separation happens in the vertical direction, caused by the $\vec{\nabla}B$ and curvature drifts. The more the density structures stay aligned with the horizontal direction, the more the turbulent transport will be effective. From this simple explanation we can deduce that the linear growth rate of a bad curvature instability, as the interchange one, has a maximum for a particular value of the magnetic shear. Both linear and non-linear gyrokinetic simulations in simplified geometry have confirmed this trend (see [10],[11]) for ITG instability which has the same type of driving mechanism as the interchange turbulence observed in the simulations. Analyzing the shape of the blobs near the separatrix in our simulations, we find turbulent structures which get more and more tilted with respect to the horizontal direction for increasing magnetic shear, as one can see in figure 4.

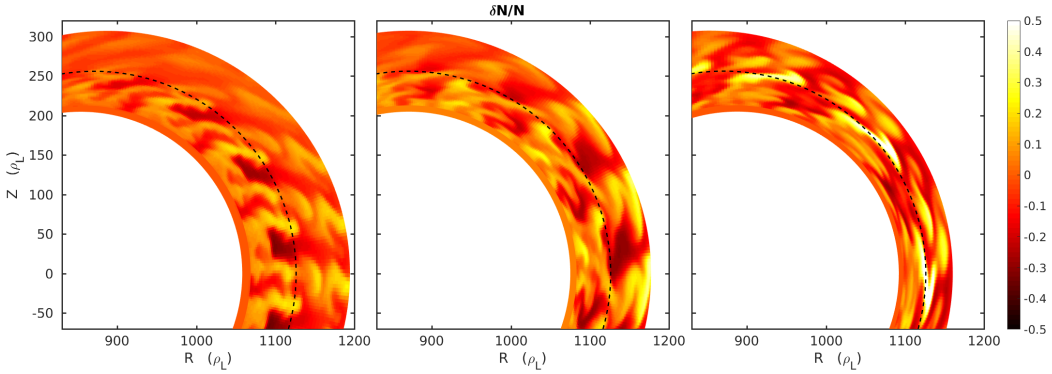

Figure 4: Snapshot of the density structures in the region between Low-field side and the top of the simulated tokamak. From left to right, the Inner shift, No shift and Outer shift case.

In particular, in the cases with a more elevated shear, the structures tend to stay aligned to the horizontal direction only for a smaller poloidal span. It is plausible so, that the elevated shear values which characterize our turbulence simulations are larger than the optimum value for the turbulence development, and so that a higher magnetic shear leads to an improved stability. This picture is consistent with our simulation results.
The magnetic shear effect, nevertheless, is not limited to a purely geometric feature. Indeed it is known to act in synergy with the $E \times B$ shear, as pointed out in [12]. This analysis would thus need a further scan in the magnetic shear parameter for the three shown cases, in order to build the stability curve appropriately. This goes beyond the scope of the present paper.

4.3 Collisional transport

Collisional transport, which is modeled in TOKAM3X with a diffusive laplacian operator in density equation, is a possible candidate for the turbulence stabilization, as it gives a negative contribution to the linear growth rate in the linear stability analysis[7]. In our model the destabilizing term for turbulence, as shown by equation (4), is related to a gradient of the first order in the physical space. The diffusive term implies instead a second order derivative in space. The relative weight of the destabilizing and the collisional term is thus locally affected by the distance between the flux surfaces. When compressing the flux surfaces, for example, the destabilizing term grows pro-

portionally to the flux surface gradient, while the diffusive ones grow with a quadratic trend. Thus the effectiveness of the collisional transport grows with the flux compression, and a steeper pressure gradient could be needed to drive the turbulence. At LFS midplane, where the majority of the turbulent cross-field flux is concentrated, in the outer shift case the flux surfaces are more compressed by a factor of two with respect to the inner shift case. We expect so a more efficient collisional transport, and so a higher turbulence stabilization, in the outer shift case.
In order to evaluate this effect, two simulations have been run with a simple limiter geometry, without any Shafranov shift, varying the diffusion coefficient. This procedure has been chosen in order to simulate artificially the local increase (or decrease, depending on the flux expansion value) of diffusion coefficient described above. In the first simulation the diffusion coefficient has been divided by a factor 5, while in the second it has been multiplied by a factor 5.
This modulation of the diffusion coefficient value has not shown evidence of any remarkable changes in the average density profiles. This result is reassuring, since one of the hypothesis underneath the TOKAM3X physical model consists of the negligibility of the collisional diffusive transport with respect to the convective one. We are now sure that the simulations with the three different magnetic equilibria are in a parameter region where the collisional transport has a negligible impact. However, the interpolation scheme used in the code could induce a small numerical diffusion whose evaluation is more challenging, and cannot be totally excluded.

5 SOL paralell flow analysis

An analysis of the parallel flows in the SOL is useful to have a more complete picture of the global equilibrium. Figure 5 shows the poloidal profiles of the parallel Mach number resulting from the simulations, at a flux surface in the middle of the SOL.

We can see from figure 5 that the trends in parallel Mach number poloidal profiles are very similar. In particular, the stagnation point is very close to the LFS midplane and almost coincides for the three cases. According to the model presented in [13], this tells us that the center of mass of the particle

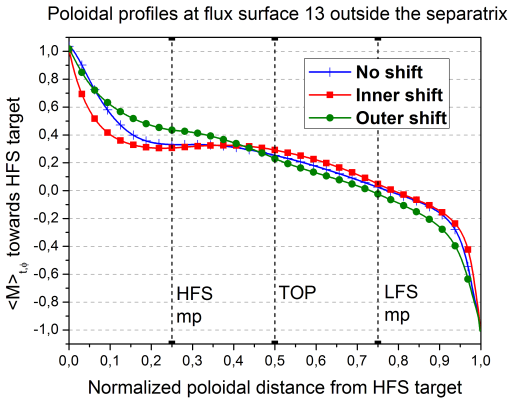

Figure 5: Poloidal profile of the parallel Mach number at a specific flux surface in the Scrape-Off Layer

source in the SOL is placed at the LFS midplane. This confirms the fact that the interchange turbulence is the main driver for the parallel flow in the SOL. Mach profile in the outer shift case shows a slight difference with respect to the other cases, mainly far from the stagnation point. In particular, the parallel Mach number is higher in absolute value in these regions. From the model presented in [13], we know that what determines the Mach number is the distribution along the parallel direction of the particle source. Since the safety factor, as explained before, is lower for the outer shift configuration, a fixed poloidal displacement results in a smaller path in the parallel direction. So even if the poloidal distribution of the cross-field flux, which is the particle source for the parallel flows, is similar, its profile along the parallel direction is different. More specifically, the particle source results more localized in the parallel direction with respect to the other geometries, resulting in higher Mach number values far from the stagnation point.

6 Conclusion

TOKAM3X 3D global turbulence simulations are run using three analytical magnetic equilibria characterized by different flux expansions at the LFS midplane. Turbulent fluxes across the flux surfaces have been studied, re-

ferring to magnetic coordinates which are independent of the flux expansion itself. The resulting fluxes have a similar poloidal distribution, due to the dominant interchange mechanism, and a comparable amplitude, due to the fact that the system is driven by a fixed source. Steeper density gradients along the magnetic coordinate are found in the case of outer shift, so when flux surfaces are more compressed at the LFS midplane, denoting an improvement in turbulence stabilization. The case without shift presents an intermediate situation, and the case where the maximum of the flux expansion is situated at the LFS midplane shows the flattest gradients. In order to explain this, the curvature term g, which locally drives the turbulence, is averaged over the parallel direction. Results show that, in the case with flux expansion concentrated at the LFS midplane, particles cover a longer parallel path in a favourable region for the instability: this comes both from the shift of the flux surfaces itself and from the higher safety factor q at the LFS midplane. Macroscopic differences are also found in the magnetic shear parameter, calculated at the LFS midplane. A stronger magnetic shear in the case of weaker flux expansion at LFS midplane is believed to help in the dissipation of the turbulent structures, improving thus the stabilization.
Globally, the simulations disclose the importance of the magnetic geometry in the determination of the turbulent cross-field transport. There is an interesting interplay between features linked to the physical space and to the magnetic one, since the variations in the real space of magnetic features, as the toroidal field or the safety factor, play a fundamental role in driving the turbulence. A variation in the flux expansion affects both the geometrical and magnetic characteristics, thus conditioning the overall equilibrium.
Results are in line with similar simulations found in the literature, that already underlined the importance of flux expansion and magnetic shear for the blob propagation [3]. In divertor geometry, the described effects are likely to be greatly enhanced. In this magnetic configuration indeed, the flux expansion presents a strong poloidal variability, notably between the LFS midplane and the X-point region. Higher values of magnetic shear at the midplane, as defined in the previous section, are achieved, because of the presence of the X-point. Taking into account all these aspects, the divertor configuration should lead to to a higher turbulence stabilization, taking to extreme the case of the outer shift. The presented work, putting in evidence the effects of the flux expansion on turbulent transport, will allow thus to better understand the simulations run in divertor configuration.

Acknowledgements

This work has been carried out within the framework of the EUROfusion Consortium and has received funding from the Euratom research and training programme 2014-2018 under grant agreement No 633053 (projects WP14/ER/CEA09 and WP15/ENR01/EPFL-05). The views and opinions expressed herein do not necessarily reflect those of the European Commission. The authors would like to thank the financial support by the AMIDEX project KFC.

References

[1] P. Tamain, H. Bufferand, G. Ciraolo, C. Colin, D. Galassi, Ph. Ghendrih, F. Schwander, and E. Serre. The TOKAM3X code for edge turbulence fluid simulations of tokamak plasmas in versatile magnetic geometries. *J. Comp. Phys.*, 2016.

[2] D. Galassi, P. Tamain, H. Bufferand, G. Ciraolo, Ph. Ghendrih, C. Baudoin, C. Colin, N. Fedorczak, N. Nace, and E. Serre. Drive of parallel flows by turbulence and large-scale e b transverse transport in divertor geometry. *Nuclear Fusion*, 57(3):036029, 2017.

[3] N. R. Walkden, B. D. Dudson, and G. Fishpool. Characterization of 3D filament dynamics in a MAST SOL flux tube geometry. *Plasma Phys. Control. Fusion*, 55:105005, 2013.

[4] C. Baudoin, P. Tamain, G. Ciraolo, R. Futtersack, A. Gallo, P. Ghendrih, Y. Marandet, N. Nace, and C. Norscini. On the effect of electron temperature fluctuations on turbulent heat transport in the edge plasma of tokamaks. *Contributions to Plasma Physics*, 56(6-8):563–568, 2016.

[5] S. I. Braginskii. Transport Processes in a Plasma. *Reviews of Plasma Physics*, 1:205, 1965.

[6] F. Schwander, G. Chiavassa, G. Ciraolo, Ph. Ghendrih, L. Isoardi, A. Paredes, Y. Sarazin, E. Serre, and P. Tamain. Parallel shear flow instability in the tokamak edge. *J. of Nucl. Mat.*, 415(1, Supplement):S601 – S604, 2011. Proceedings of the 19th International Conference on Plasma-Surface Interactions in Controlled Fusion.

[7] P. Tamain. Etude des flux de matière dans le plasma de bord des tokamaks : Alimentation, transport et turbulence. *Ph.D. Thesis*.

[8] J. Wesson. *Tokamaks*. Oxford University Press, 2004.

[9] T. M. Antonsen, J. F. Drake, P. N. Guzdar, A. B. Hassam, Y. T. Lau, C. S. Liu, and S. V. Novakovskii. Physical mechanism of enhanced stability from negative shear in tokamaks: Implications for edge transport and the L-H transition. *Phys. Plasmas*, 3(6):2221, 1996.

[10] R. E. Waltz, G. M. Staebler, W. Dorland, G. W. Hammett, M. Kotschenreuther, and J. A. Konings. A gyro-Landau-fluid transport model. *Phys. Plasmas*, 4(7):2482, 1997.

[11] C. Bourdelle, G.T. Hoang, X. Litaudon, C.M. Roach, T. Tala, ITPA Group, and the International ITB Database Work. Impact of the α parameter on the microstability of internal transport barriers. *Nucl. Fusion*, 45(2):110–130, feb 2005.

[12] N. Fedorczak, Ph. Ghendrih, P. Hennequin, G. R. Tynan, P. H. Diamond, and P. Manz. Dynamics of tilted eddies in a transversal flow at the edge of tokamak plasmas and the consequences for LH transition. *Plasma Phys. Control. Fusion*, 55(12):124024, dec 2013.

[13] J. P. Gunn, C. Boucher, M. Dionne, V. Fuchs, T. Loarer, J. Sto, I. Nanobashvili, R. Pa, J. Ada, J. Bucalossi, R. Dejarnac, T. Van. Rompuy, R. Zago, P. Devynck, P. Hertout, M. Hron, G. Lebrun, P. Moreau, F. Rimini, A. Sarkissian, and G. Van. Oost. Evidence for a poloidally localized enhancement of radial transport in the scrape-off layer of the Tore Supra tokamak. *J. Nucl. Mater.*, 365:484–490, 2007.